physica status solidi

pss

www.pss-journals.com

reprint

WILEY-VCH

Phys. Status Solidi C **12**, No. 6, 822–825 (2015) / **DOI** 10.1002/pssc.201400338

physica status solidi c
www.pss-c.com
current topics in solid state physics

Metallic conductivity and weak antilocalization in $Bi_2Te_{2.7}Se_{0.3}$ thin films

Nadir A. Abdullayev[*,1], Afet M. Kerimova[,1], Khayala V. Aliquliyeva[1], Yong Gu Shim[2], Kojiro Mimura[2], Kazuki Wakita[3], Oktay Z. Alekperov[1], Nazim T. Mamedov[1], and Vladimir N. Zverev[4]**

[1] Institute of Physics, Azerbaijan National Academy of Sciences, H. Javid Ave. 131, Baku-1143, Azerbaijan
[2] Osaka Prefecture University, 1-1 Gakuen-cho, Naka-ku, Sakai 599-8531, Japan
[3] Chiba Institute of Technology, 2-17-1 Tsudanuma, Narashino, Chiba 275-0016, Japan
[4] Institute of Solid State Physics, 142432, Chernogolovka, Moscow district, Russia

Received 14 October 2014, revised 17 March 2015, accepted 17 March 2015
Published online 27 April 2015

Keywords weak antilocalization, thermoelectric efficiency, surface conductivity, topological insulator, spin-orbit coupling

* Corresponding author: e-mail abnadir@physics.ab.az
** e-mail afet.kerimova@physics.ab.az

Submicron thin films of $Bi_2Te_{2,7}Se_{0,3}$ solid solution is synthesized by thermal vacuum evaporation. The films are then subjected to after-growth vacuum annealing and characterized using X-ray diffraction and confocal laser microscopy techniques. Electron transport in the synthesized films is studied over the temperature range of 1.4-300 K at magnetic fields up to 8 T. Electron localization due to electron-electron interaction, along with weak anti-localization effect at weak magnetic fields and temperatures below 8 K is observed. The latter effect is commonly encountered in thin films of topological insulators grown by molecular beam epitaxy and has therefore been ascribed to the manifestation of the topological surface states. Finally, phase coherence length is estimated.

1 Introduction

The $A_2^VB_3^V$ compounds continue to attract much attention for their thermoelectric properties with thermoelectric efficiency zT ~ 1. Furthermore, they have recently been utilized as topological insulators**.**

A possible means of attaining superior thermoelectric efficiency (zT >> 1) in two-dimensional systems [1-3] is causing especial interest in thin film varieties of $A_2^VB_3^V$.

In contrast to bulk-material-based devices, thin-film-based Bi_2Te_3 or Bi_2Se_3 thermoelectrics allow for substantial cooling to 32 K and thermal flow circulation up to 700 W/cm^2 [4]. At the same time, local cooling or heating occurs at a rate that is several orders of magnitude faster.

However, the most important issue directly related to our present studies is that the topological surface electron states in thin films can be more easily accessed because the contribution of the bulk (volumetric) carriers in the thin film case is significantly reduced. This has been vividly exposed in numerous of the recent works on Bi_2Se_3 thin films obtained by molecular beam epitaxy (MBE) [5-9].

The objective of this work was to examine whether thin films that are less perfect than those obtained by MBE still preserve their topological properties. $Bi_2(Te_{0.9}Se_{0.1})_3$ solid solution was selected as the core material for these studies for the following reasons. The first is that a solid solution is always structurally more disordered than terminate compounds. The other is that the $Bi_2(Te_{0.9}Se_{0.1})_3$ composition exhibits the best thermoelectric properties among the materials of the Bi_2Te_3-Bi_2Se_3 system [10, 11].

Here we report the obtained results on charge transport in $Bi_2(Te_{0.9}Se_{0.1})_3$ thin films grown by the cheap hot wall method.

2 Preparation of films, their structure, and experimental details

$Bi_2(Te_{0.9}Se_{0.1})_3$ was synthesized by melting highly pure chemical constituents in evacuated quartz ampoules in a rotary furnace at T ~ 800 °C with subsequent cooling under the furnace-off condition. The films were obtained by "hot wall" thermal vacuum evaporation of the synthesized substance onto glass substrates. The substrate was held at a

constant temperature of 300 °C. The thickness of the obtained films varied between 500 and 600 nm. Thermal annealing of the obtained films was performed in vacuum at T = 200 °C, 300 °C and 400 °C for 1 h.

Figure 1 displays the X-ray diffraction (XRD) patterns of the as-grown film (bottom curve) and those of the film after annealing at 200 °C (top curve). As can be seen, XRD reflexes of the annealed film are more intense.

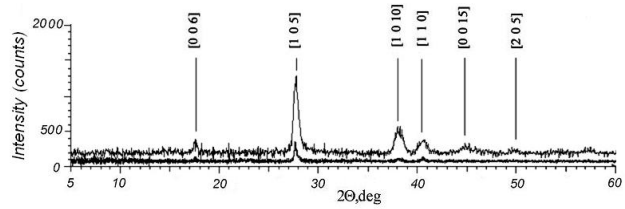

Figure 1 X-ray diffraction patterns of as-grown film (bottom curve) and thin film after annealing at 200 °C (top curve).

The observed reflexes confirm that the structure of crystallites in the obtained film is rhombohedral with space group R3m. Such structure is common for all compounds of the Bi_2Se_3-Bi_2Te_3 family [12].

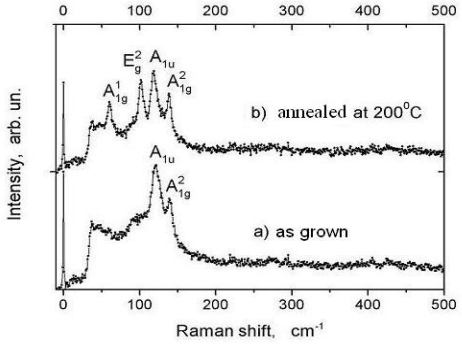

Figure 2 Raman spectra of $Bi_2(Te_{0.9}Se_{0.1})_3$ thin films.

Raman spectra obtained from the above films in backscattering geometry are shown in Fig. 2. Two Raman lines that correspond to A_{1u}^2 (120 cm^{-1}) and A_{1g}^2 (138 cm^{-1}) lattice modes are observed in as-grown $Bi_2(Te_{0.9}Se_{0.1})_3$ films (bottom curve). The presence of the IR-active mode A_{1u}^2 in the Raman spectrum indicates a break in symmetry that can be due to stacking faults or mechanical stress.

The remarkable feature of the Raman spectrum of the annealed film (Fig. 2, top curve) is the emergence of two more lines as compared to the spectrum of the non-annealed film (Fig. 2, bottom curve). These lines can be identified as E_g^2 (102 cm^{-1}) and A_{1g}^1 (60 cm^{-1}). The emergence of these modes is further evidence of more complete crystallization of the films subjected to vacuum annealing. Note that the values of phonon frequencies obtained in this study are consistent with the experimental and calculated data for bulk single crystals [12].

The electrical conductivity of the obtained films was studied in a wide range of temperature (1.4-300 K) and magnetic fields (up to 8 T). Measurements were taken using the standard four-probe method and selective detection technique at a frequency of ≈20.5 Hz. Ohmic silver paste point contacts were used.

3 Experimental results and discussion

The temperature dependence of the resistivity of as-grown thin film is shown in Fig. 3a. The as-grown thin film exhibits thermally activated semiconductor-type conduction that is due to the disordered structure of the film. On the other hand, the same film subjected to vacuum annealing at 200 °C exhibits metallic-type conductivity similar to Bi_2Se_3-Bi_2Te_3 bulk single crystals (Fig. 3b).

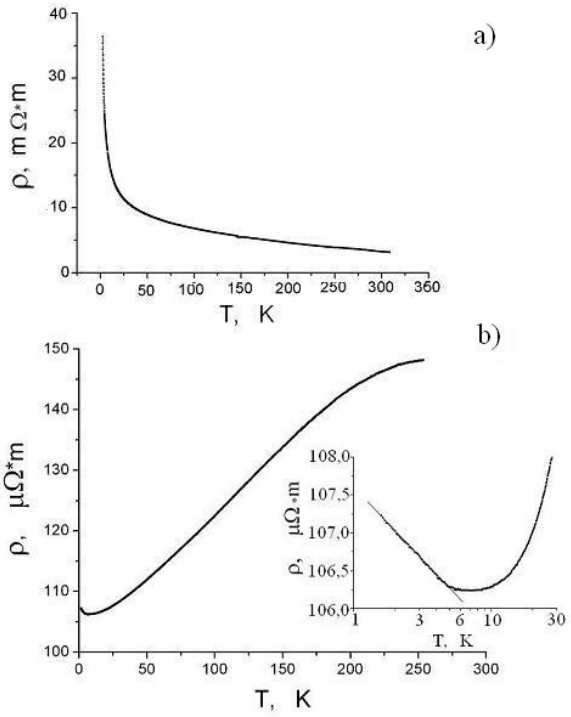

Figure 3 Temperature dependence of the resistivity in $Bi_2(Te_{0.9}Se_{0.1})_3$ thin films: (a) as grown, (b) annealed at 200 °C. Inset: low-temperature part.

The fact that the resistivity at low temperatures increases logarithmically as temperature decreases below 8 K (Fig. 3b, insert) is of key importance because it indicates weak localization, which is typical for disordered metals [13]. Note that the above temperature dependence of the resistivity and weak localization effect are always accompanied by negative magnetoresistivity when observed in bulk $A_2^VB_3^{VI}$ single crystals.

The Hall and magnetoresistivity data for annealed $Bi_2Te_{2.7}Se_{0.3}$ thin films are shown in Fig. 4a and 4b, respectively. According to the obtained Hall data, our $Bi_2(Te_{0.9}Se_{0.1})_3$ thin film is n-type, with electron concentration n ~ 10^{19} cm^{-3} and mobility μ~100 cm^2/V·s at T ~ 4.2 K.

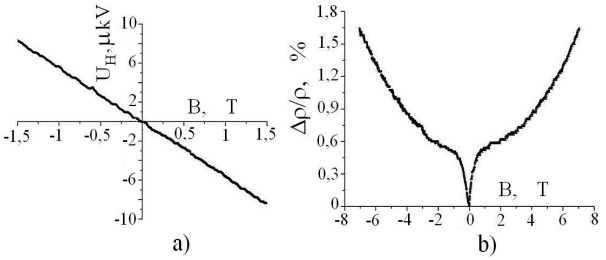

Figure 4 Hall (a) and magnetoresistivity (b) measurements in annealed $Bi_2Te_{2.7}Se_{0.3}$ thin films.

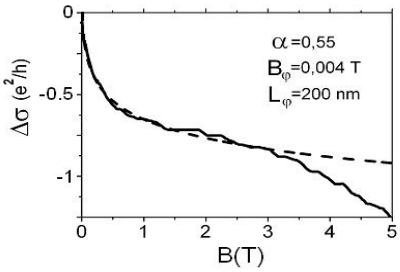

Figure 5 The magnetic field dependence of the magnetoconductivity (dashed curve, theoretical calculations).

In magnetic fields above 1 T, the magnetoresistivity is described by a standard Lorentz quadratic field dependence inherent in $A_2^{V}B_3^{VI}$ single bulk crystals (Fig. 4b). However, a sharp feature with a drastic increase in the magnetoresistivity upon increasing the magnetic field near B = 0 is observed in a region below B < 1 T (Fig. 4b). The sharp dip in the magnetic field dependence of magnetoresistivity is a typical manifestation of weak antilocalization (WAL) and has been observed in thin films, microflakes, and nanowires of several topological insulators [5-9, 14, 15]. In bulk specimens of topological insulators WAL does not appear because of the overwhelming contribution of the bulk carriers. WAL itself is inherent in electron transport of a Berry's phase associated with the conical surface states [16].

Studies of the film thickness dependence of WAL [6] have shown that WAL weakens with increasing film thickness and completely disappears at thicknesses above 1 μm.

The fact that we observe WAL in relatively thick thin-films (~500 nm) of a solid solution of a topological insulator is another indication of the topological nature of the electronic states involved. Topological states are protected against disturbances that do not break time reversal symmetry and, are therefore robust. Note that the strong spin-orbit interaction is a very important prerequisite for the formation of topological surface states.

If strong spin-orbit interaction ($\tau_\phi >> \tau_{so}, \tau_e$) is considered, theoretical magnetic field dependence of the variation of magnetoconductance in the 2D limiting case is described by Hikami-Larkin-Nagaoka (HLN) [17]:

$$\Delta\sigma(B) = -\alpha\frac{e^2}{\pi h}\left[\psi\left(\frac{1}{2}+\frac{B_\varphi}{B}\right)-\ln\left(\frac{B_\varphi}{B}\right)\right], \qquad (1)$$

where τ_{so} (τ_e) is the spin-orbit (elastic) scattering time, ψ is the digamma function, $B_\phi = \hbar/(4De\tau_\phi)$ is a characteristic field related to the dephasing time τ_ϕ, D is the diffusion constant, and h is the Planck constant. If we consider that $D\tau_\varphi = L_\varphi^2$, where L_φ is the phase coherence length, then $B_\varphi = \hbar/(4eL_\phi^2)$. The coefficient α is 1/2 in the WAL-dominant case.

Figure 5 shows the results of fitting the HLN Eq. (1) to our experimental data. The best agreement between the experimental data (solid curve) and results of calculation (dashed curve) is observed for $\alpha = 0.55$ and the characteristic field $B_\phi = 0.004$ T. The value $\alpha = 0{,}55$ is very close to the expected $\alpha = 0.5$. Given $B_\varphi = \hbar/(4eL_\phi^2) = 0.004$ T, the value of L_φ is estimated to be 200 nm. This last value is comparable with the thickness (L ~ 500 nm) of the studied films. Thus, in our case, the overwhelming contribution of the electron transport through surface states in total conductivity can be expected for film thickness d << 200 nm.

Thus, we have two facts that are seemingly in conflict with each other. A negative cusp in magnetoconductivity is indicative of the presence of topological surface states which are protected from localization and exhibit weak antilocalization. At the same time, the low temperature conductivity shows logarithmic increase with lowering temperature, which is typical for disordered metals and is attributed to the weak localization. As recently shown by Lu and Shen [18] who studied conductivity for massless and heavy fermions, the above conflicting facts can be explained if the electron-electron interaction and quantum interference are considered simultaneously. In this case, it explicitly turns out that the temperature dependence of the conductivity is dominated by the interaction, while the magnetoconductivity is mainly affected by the quantum interference.

4 Conclusions

We have studied the electrical resistivity of as-grown and vacuum-annealed thin films of $Bi_2(Te_{0.9}Se_{0.1})_3$ solid solution in a wide range of temperatures and magnetic fields. Only the vacuum-annealed thin films showed electrical properties reasonably similar to those of bulk crystals. Both weak localization and weak antilocalization occurred, the latter being uniquely inherent in topological insulators. Unusually for weak antilocalization, the logarithmic growth of resistivity with decreasing temperature below 8 K has been ascribed to the dominant contribution of electron-electron scattering processes in low-temperature electron transport.

There are two issues that seem to be worthy of mentioning again. The first is the applied thin-film deposition method (hot wall). The second is the solid solution as a subject of studies. As far as the employed deposition tech-

nology is rougher than MBE and the solid solution is a more disordered system in comparison with terminate compound, the scattering of charge carriers is strong. Even under these unfavorable conditions we observe a quantum transport signature of the topological surface states.

Acknowledgements This work was supported by the Science Development Foundation under the President of the Republic of Azerbaijan, Grant No. EIF-2012-2(6)-39/01/1.

References

[1] L. D. Hicks and M. S. Dresselhaus, Phys. Rev. B **47**, 12727 (1993).
[2] L. D. Hicks, T. C. Harman, and M. S. Dresselhaus, Appl. Phys. Lett. **63**, 3230 (1993).
[3] L. D. Hicks and M. S. Dresselhaus, Phys. Rev. B **47**, 16631 (1993).
[4] R. Venkatasubramanian, E. Sivola, T. Colpitts, and B. O'Quinn, Nature **413**, 597 (2001).
[5] J. Chen, H. J. Qin, F. Yang, J. Liu, T. Guan, F. M. Qu, G. H. Zhang, J. R. Shi, X. C. Xie, C. L. Yang, K. H. Wu, Y. Q. Li, and L. Lu, Phys. Rev. Lett. **105**, 176602 (2010).
[6] Y. S. Kim, M. Brahlek, N. Bansal, E. Edrey, G. A. Kapile vich, K. Iida, M. Tanimura, Y. Horibe, S. W. Cheong, and S. Oh, Phys. Rev. B **84**, 073109 (2011).
[7] M. Liu, J. Zhang, C. Chang, Z. Zhang, X. Feng, K. Li, K. He, L. Wang, X. Chen, X. Dai, Z. Fang, Q. Xue, X. Ma, and Y. Wang, Phys. Rev. Lett. **108**, 036805 (2012).
[8] Y. Takagaki, B. Jenichen, U. Jahn, M. Ramsteiner, and K.-J. Friedland, Phys. Rev. B **85**, 115314 (2012).
[9] H. He, G. Wang, T. Zhang, I. K. Sou, G. K. L. Wong, J. N. Wang, H. Z. Lu, S. Q. Shen, and F. C. Zhang, Phys. Rev. Lett. **106**, 166805 (2011).
[10] V. A. Kutasov, L. N. Lukyanova, and P. P. Konstantinov, Phys. Solid State **42**, 2039 (2000).
[11] L. V. Prokofeva, D. A. Pshenai-Severin, P. P. Konstantinov, and A. A. Shabaldin, Semiconductors **43**, 973 (2009).
[12] W. Richter, H. Kohler, and C. R. Becker, Phys. Status Solidi B **84**, 619 (1977).
[13] A. A. Abrikosov, Fundamentals of the Theory of Metals (North-Holland, 1988).
[14] S. P. Chiu and J. J. Lin, Phys. Rev. B **87**, 035112 (2013).
[15] B. Hamdou, J. Gooth, A. Dorn, E. Pippel, and K. Nielsch, Appl. Phys. Lett. **102**, 223110 (2013).
[16] L. Fu and C. L. Kane, Phys. Rev. B **76**, 045302 (2007).
[17] S. Hikami, A. I. Larkin, and Y. Nagaoka, Prog. Theor. Phys. **63**, 707 (1980).
[18] H. Z. Lu and S. Q. Shen, Phys. Rev. Lett. **112**, 146601 (2014).